in which CrR^{2+} undergoes one-electron oxidation.

It would be desirable to consider these rates also from the standpoint of the Marcus correlation. Unfortunately, however, the necessary reduction potentials and self-exchange rates of the CrR^{3+}/CrR^{2+} couples are not yet known.

Subsequent Reactions of CrR^{3+}. The formation of an ethyl radical from the rapid unimolecular homolysis of the oxidized intermediate $CrCH_2CH_3^{3+}$ is supported by two experiments. First, the product identified by GC as ethyl bromide is readily accounted for by the reaction of the free radical with $(NH_3)_5CrBr^{2+}$, eq 10, for which precedents have been established. Second, the doubling of the rate constant (eq 8 vs. eq 11) noted when the quencher $(NH_3)_5Co(py)^{3+}$ is used, is consistent with the reaction of the radical with $Ru(bpy)_3^{3+}$, analogous to the known reaction of the radical with $Ru(phen)_3^{3+}$.[23]

On the other hand, we doubt that the oxidized complex $CrCH_2OCH_3^{3+}$ undergoes homolysis. More likely, it undergoes an internal electron-transfer reaction, eq 13. This is what happens when (what we presume to be) the same species is formed in the reaction with NO^+ [14] and also by milder oxidizing agents such as Cu^{2+}, Fe^{3+}, and Hg^{2+}.[13] This mode of reaction would yield Cr_{aq}^{2+} and CH_3OCH_2OH, and the latter would decompose to formaldehyde and methanol. Indeed, in the NO^+ reaction, the Cr^{2+} product of the reaction was identified and quantitatively determined.[14] In the present case the intermediate Cr^{2+} is trapped by the quencher when it is $(NH_3)_5CoBr^{2+}$ but accumulates in preference to oxidation by $Ru(bpy)_3^{3+}$ when the relatively unreactive quencher $(NH_3)_5Co(py)^{3+}$ is used. In keeping with that, the rate of reduction of $Ru(bpy)_3^{3+}$ by $CrCH_2OCH_3^{2+}$ is very nearly[29] the same for both cobalt(III) quenching complexes.

Experimental Section

Reagents. The organochromium complexes were prepared according to the procedures described in other publications.[11-14] The complex $[Co(NH_3)_5py](OSO_2CF_3)_3$ was prepared from the reaction between pyridine (distilled from KOH) and the inner-sphere triflato-pentaammine complex. The preparation of the latter has been described in the literature.[33] Other chemicals were available from earlier work or from commercial sources.

Procedures. The laser flash photolysis system was based on one described in the literature[34] and has been detailed previously.[35] In brief, the procedure was as follows. The photolytic excitation of $Ru(bpy)_3^{2+}$ was provided by a 600-ns pulse from a Phase-R Model DL-1100 dye laser (coumarin dye, emission at 460 nm) that impinged on a solution contained in a quartz fluorescence cuvette. The subsequent optical changes were monitored at right angles to the exciting pulse. The signal from the photomultiplier tube was collected by using a Nicolet digitizing oscilloscope interfaced to an Apple II+ microcomputer. A typical laser pulse kinetics experiment was performed on a solution containing $[Ru(bpy)_3]Cl_2$ (12-26 μM), the cobalt(III) quencher, usually $[Co(NH_3)_5Br](ClO_4)_2$ (2-10 mM), and the CrR^{2+} complex (20 μM-2 mM). These solutions were maintained at ionic strength 0.10 M by addition of perchloric or hydrochloric acid. The rate constants were independent of $[H^+]$ in this narrow range and were the same for Cl^- and ClO_4^- solutions. The transmittance data, converted to absorbance values that, with one exception, followed first-order kinetics for 3 half-lives. For reasons not ascertained, the reaction of the complex $CrCH_2C_6H_4$-*p*-CH_3^{2+} followed biphasic kinetics, which were deconvoluted by standard methods. The first (faster) reaction responds to the proper concentration variables and is presumed to be the process of interest.

The analysis for the organic product(s) of the reaction between $Ru(bpy)_3^{3+}$ and $CrCH_2CH_3^{2+}$ was carried out. This was done in an experiment in which the Ru(III) complex was generated by continuous photolysis of a stirred solution containing $Ru(bpy)_3^{2+}$ (56 μM), $(NH_3)_5CoBr^{2+}$ (0.01 M), and $CrCH_2CH_3^{2+}$ (5.0 mM) in a cell having a jacket containing 0.01 M $(NH_3)_5CoBr^{2+}$ (to act as a filter of the UV light so that the products derived from photolysis of the ruthenium complex, not the cobalt quencher). The cell was irradiated for 4 min with a 275-W sunlamp placed 14 cm away. After a sufficient time (4 h) for the remaining ethylchromium(2+) ion to decompose to ethane by acidolysis, the reaction mixture was analyzed by gas chromatography on a 10% FFAP column. The result, in comparison with standards, established the only organic product to be ethyl bromide.

Acknowledgment. This work was supported by the U.S. Department of Energy, Office of Basic Energy Sciences, Chemical Sciences Division, under Contract W-7405-Eng-82.

Registry No. $(H_2O)_5Cr$-*p*-$CH_2C_6H_4CH_3^{2+}$, 53150-36-0; $(H_2O)_3CrCH_2C_6H_5^{2+}$, 34788-74-4; $(H_2O)_5Cr$-*p*-$CH_2C_6H_4CF_3^{2+}$, 53150-38-2; $(H_2O)_5Cr$-*p*-$CH_2C_6H_4CN^{2+}$, 53150-39-3; $(H_2O)_5CrCH_2OCH_3^{2+}$, 78402-17-2; $(H_2O)_5CrCH(CH_3)_2^{2+}$, 60764-48-9; $(H_2O)_5CrCH_2CH_3^{2+}$, 52653-39-1; $(H_2O)_5CrCH_3^{2+}$, 32108-96-6; $(NH_3)_5Co(py)^{3+}$, 31011-67-3; $(NH_3)_5CoBr^{2+}$, 14970-15-1; $Ru(bpy)_3^{3+}$, 18955-01-6.

(33) Kupferschmidt, W. C.; Jordan, R. B. *Inorg. Chem.* **1982**, *21*, 2089.

(34) Hoselton, M. A.; Lin, C.-T.; Schwartz, H. A.; Sutin, N. *J. Am. Chem. Soc.* **1978**, *100*, 2383.

(35) Connolly, P.; Espenson, J. H.; Bakac, A. *Inorg. Chem.*, in press.

Contribution from the Department of Chemistry, Iowa State University, Ames, Iowa 50011

Characterization of the Structure, Properties, and Reactivity of a Cobalt(II) Macrocyclic Complex

Andreja Bakač,* Mark E. Brynildson, and James H. Espenson*

Received April 22, 1986

The cobalt(II) macrocycle $L_2Co(dmgBF_2)_2$ has been characterized by crystallography (L = CH_3OH) and by spectroscopic UV/vis, EPR, electrochemical, and magnetic methods as well as elemental analysis for L = H_2O. The complex $(CH_3OH)_2Co(dmgBF_2)_2$ crystallizes in the triclinic space group $P\bar{1}$ with one molecule in a cell of dimensions a = 7.955 (6) Å, b = 8.180 (6) Å, c = 7.918 (6) Å, α = 99.55 (2)°, β = 118.13 (2)°, and γ = 66.52 (2)°. The data refined to a final value of the weighted R factor of 0.046 based on 1027 independent observations. It is a six-coordinate, low-spin complex (μ = 1.92 μ_B), showing substantial elongation of the axial Co-O bonds (2.27 Å). In aqueous perchloric acid the diaquo complex is reversibly oxidized to $(H_2O)_2Co(dmgBF_2)_2^+$ by Fe^{3+}. The equilibrium constant is 34.7 (25 °C), yielding $E°$ = 0.65 V vs. NHE for the Co(III)/Co(II) couple. The second-order rate constant for the forward reaction has the value $k_f/M^{-1}\,s^{-1} = 2.9 \times 10^2 + 1.2 \times 10^2[H^+]^{-1}$. The prominent inverse-$[H^+]$ component suggests an inner-sphere reaction between $(H_2O)_5FeOH^{2+}$ and the Co(II) complex. A detailed analysis of the mechanism interpreted on that basis is presented; it suggests that intramolecular electron transfer within a binuclear intermediate is the rate-limiting step.

Introduction

In spite of extensive earlier investigations, complexes of cobalt with macrocyclic ligands continue to be actively studied. They hold continued interest not only because of their relationship to the intriguing chemistry of vitamin B_{12},[1-3] but also because they offer a wide variety of chemistry within a family of well-defined

(1) Lenhart, P. G.; Hodgkin, D. C. *Nature (London)* **1962**, *192*, 937.

0020-1669/86/1325-4108$01.50/0

and seemingly narrowly constrained chemical substances. The macrocyclic complexes exhibit some distinct contrasts to related complexes containing monodentate and bidentate ligands. For example, they form alkyl complexes that are stable and isolable, they show enhanced rates of self-exchange, electron-transfer, and ligand-exchange reactions, and most are known in oxidation states I–III.[4,5]

Although these complexes form from Co(II) salts with high formation constants, many bind O_2 or are oxidized by it. Also at high $[H^+]$, such as 0.01–1 M, many of the Co(II) macrocycles rapidly decompose to Co_{aq}^{2+}. These characteristics limit their general utility in certain applications, most notably in reactions that must be carried out in acidic media.

In contrast to such patterns[6,7] the complex[8] $(H_2O)_2Co(dmgBF_2)_2$ (see structural formula) is remarkably resistant to both reactions. In addition to its earlier use as a model complex for

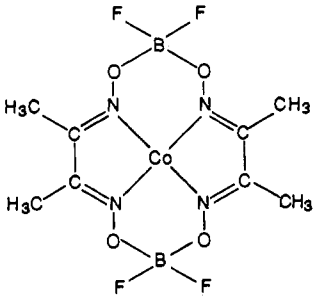

vitamin B_{12},[9-11] the same complex in the Co(II) oxidation state is proving to be a desirable substrate in several areas, for example, in studies of homolytic substitution reactions of alkyl complexes[12] and in redox reactions with inorganic substrates.[13] We were thus motivated to characterize this cobalt(II) complex fully. We report here the details of its preparation and characterization by spectroscopic (UV/vis, EPR), magnetic, and structural methods (X-ray crystal structure of the bis(methanol) complex, $(CH_3OH)_2Co(dmgBF_2)_2$). We also report data from a study of the equilibrium and kinetics of its reversible electron-transfer reaction with Fe(III), from which the reduction potential for the Co(III)/Co(II) couple can be evaluated.

Experimental Section

$(H_2O)_2Co(dmgBF_2)_2$. Crystalline samples were prepared[12] as follows. A suspension of $Co(OAc)_2 \cdot 4H_2O$ (2.0 g, 8.0×10^{-3} mol) and $dmgH_2$ (1.9 g, 1.6×10^{-2} mol) in 150 mL of oxygen-free diethyl ether was treated with excess freshly distilled $BF_3 \cdot Et_2O$ (10 mL) and the mixture stirred at room temperature for 6 h, during which time the desired product precipitated. The brown solid obtained by filtration was washed several times with ice-cold water and air-dried. The purity was checked by chemical analysis and spectroscopy. Anal. Calcd for $CoC_8H_{16}O_6N_4$: Co, 14.0; C, 22.8; H, 3.80; N, 13.3. Found: Co, 14.0; C, 23.1; H, 3.78; N, 13.1.

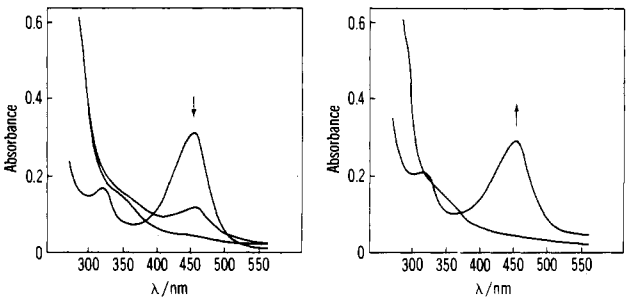

Figure 1. Initial UV/vis absorption spectrum of $(H_2O)_2Co(dmgBF_2)_2$ (left, upper spectrum, 4×10^{-5} M, 2-cm cell), which fades with time upon addition of a slight excess of Fe^{3+} (5×10^{-5} M) to that of $(H_2O)_2Co(dmgBF_2)_2^+$ (left and right, lower spectra). Prompt addition of excess Cr^{2+} restores most of the Co(II) absorption.

Other Reagents. Hydrated iron(III) perchlorate, prepared by fuming the chloride with perchloric acid, was dissolved in dilute aqueous perchloric acid to prepare stock solutions of $Fe(H_2O)_6^{3+}$. As needed, these solutions were reduced anaerobically to $Fe(H_2O)_6^{2+}$ by amalgamated zinc; the concentration of any residual $Fe(H_2O)_6^{3+}$ was determined spectrophotometrically by using thiocyanate ions. Lithium perchlorate, used for control of ionic strength, was prepared from the carbonate and recrystallized twice. Other reagents were used as purchased.

Measurements. UV/visible spectrophotometric data were obtained on a Cary Model 219 spectrophotometer having a thermostated cell compartment. Reactions too rapid for conventional spectrophotometry were followed on a Canterbury SF-3A stopped-flow spectrometer interfaced with either a Nicolet digitizing oscilloscope or the OLIS 3820 data collection system. Analysis of kinetic data was done with standard nonlinear least-squares programs.

Cyclic voltammograms were measured by use of a Bioanalytical Systems, Inc., BAS-100 electrochemical analyzer. The glass sample compartment (solution volume ~10 mL) held the three electrodes needed for cyclic voltammetry in an air-free environment. The working electrodes were a commercial hanging-mercury-drop electrode, a glassy-carbon-disk electrode (3.2-mm diameter), and a platinum-disk electrode (1.6-mm diameter). The auxiliary electrode was a platinum wire and the reference an Ag/AgCl electrode. The electrolytes used were $LiClO_4$, $HClO_4$, LiCl, or HCl.

Magnetic susceptibilities were determined by the Gouy method[14] with $[Ni(en)_3]S_2O_3$ used as the standard. EPR spectra were collected with a Bruker/IBM ER 200D-SRC spectrometer equipped with a Systron-Donner frequency counter. The probe temperature of 100–110 K was provided by cold nitrogen gas. The field was calibrated by using diphenylpicrylhydrazide (DPPH, $g = 2.0037$), MnO doped in MgO, and a NMR gaussmeter. EPR spectra were determined in a toluene–dichloromethane mixture, which produces a good glass upon freezing. Samples of $L_2Co(dmgBF_2)_2$ were prepared by dissolving the compound with L = CH_3OH in an air-free mixture of these solvents and the desired Lewis base (50:40:10, by volume). The samples, contained in a quartz EPR tube, were frozen with liquid nitrogen. Samples of the oxygen adduct $LCo(dmgBF_2)_2O_2$ were prepared by rapidly injecting an oxygen-free solution of $L_2Co(dmgBF_2)_2$, dissolved in the given base L, into an oxygen-saturated solution of toluene–dichloromethane at −50 °C. The samples were then rapidly frozen in the EPR tube by liquid nitrogen. The EPR spectra were axial in shape, and therefore the g and A values were calculated as previously described[15a,b] for cobalt(II) macrocycles.

The very limited solubility of $(H_2O)_2Co(dmgBF_2)_2$ in water makes it difficult to grow single crystals of the diaquo complex. Thus single crystals of $(CH_3OH)_2Co(dmgBF_2)_2$ suitable for X-ray diffraction were grown by the slow evaporation of a solution of $(H_2O)_2Co(dmgBF_2)_2$ dissolved in methanol. These crystals lose solvent readily, fracturing on contact with air. To prevent this, the crystal was mounted in a sealed 0.3-mm Lindemann glass capillary tube containing the mother liquor.

Diffraction data[16] were collected on a Syntex $P2_1$ four-circle X-ray diffractometer. The crystal system and orientation matrix were obtained by using an automatic indexing program.[17] The resulting triclinic re-

(2) Pratt, J. M. *Inorganic Chemistry of Vitamin B_{12}*; Academic: New York, NY, 1972.
(3) Schrauzer, G. N. *Acc. Chem. Res.* **1968**, *1*, 97.
(4) Dodd, D.; Johnson, M. D. *J. Organomet. Chem.* **1973**, *52*, 1–232.
(5) Wong, C.-L.; Switzer, J. A.; Balakrishnan, K. P.; Endicott, J. F. *J. Am. Chem. Soc.* **1980**, *102*, 5511.
(6) (a) Adin, A.; Espenson, J. H. *Inorg. Chem.* **1972**, *11*, 686. (b) Gjerde, H. B.; Espenson, J. H. *Organometallics* **1982**, *1*, 435.
(7) Schrauzer, G. N.; Lee, L. P. *J. Am. Chem. Soc.* **1970**, *92*, 1551.
(8) The compound $(H_2O)_2Co(dmgBF_2)_2$ is properly named (diaquo)bis[(difluoroboryl)dimethylglyoximato]cobalt(II). It is closely related to the so-called "cobaloximes" by the substitution of $(O–BF_2–O)^-$ for the $(O–H–O)^-$ group in the hydrogen-bonded bis(dimethylglyoximato) unit. Other ligands referred to are as follows: Me_4[14]tetraeneN$_4$ = 2,3,9,10-tetramethyl-1,4,8,11-tetraazacyclotetradeca-1,3,8,10-tetraene; Me_2[14]1,11-dieneN$_4$-13-one = 12,14-dimethyl-1,4,8,11-tetraazacyclotetradeca-1,11-dien-13-one; Me_6[14]4,11-dieneN$_4$ = 5,7,7,12,14,14-hexamethyl-1,4,8,11-tetraazacyclotetradeca-4,11-diene; Me_2[14]4,7-dieneN$_4$ = 5,7-dimethyl-1,4,8,11-tetraazacyclotetradeca-4,7-diene; Me_2pyo[14]trieneN$_4$ = 2,12-dimethyl-3,7,11,17-tetraazabicyclo-[11.3.1]heptadeca-1(17),2,11,13,15-pentaene.
(9) Schrauzer, G. N.; Sibert, J. W.; Windgassen, R. J. *J. Am. Chem. Soc.* **1968**, *90*, 6681.
(10) Schrauzer, G. N.; Sibert, J. W. *J. Am. Chem. Soc.* **1970**, *92*, 1022.
(11) Schrauzer, G. N.; Weber, J. H.; Beckman, J. M. *J. Am. Chem. Soc.* **1970**, *92*, 7078.
(12) Bakac, A.; Espenson, J. H. *J. Am. Chem. Soc.* **1984**, *106*, 5197.
(13) Brynildson, M. E.; Bakac, A.; Espenson, J. H., unpublished observations.
(14) Angelici, R. J. *Synthesis and Technique in Inorganic Chemistry*, 2nd ed.; Saunders: Philadelphia, 1977; p 46.
(15) (a) Tovrog, B. S. *Diss. Abstr. Int., B* **1976**, *36*, 4471. (b) Drago, R. S.; Tovrog, B. S.; Kitko, D. J. *J. Am. Chem. Soc.* **1976**, *98*, 5144.
(16) The structural data collection and refinement were carried out at Iowa State University's diffraction facility by J. E. Benson.
(17) Jacobson, R. A. *J. Appl. Cryst.* **1976**, *9*, 115.

Table I. EPR Parameters[a] for $(L,L')Co(dmgBF_2)_2$

L	L′	$g_\parallel$	$\lvert A_\parallel\rvert^b$	$g_\perp$	$\lvert A_\perp\rvert^b$
CH_3OH	CH_3OH	2.013	107	2.28	10
CH_3CN	CH_3CN	2.015	104	2.28	10
$(CH_3)_2CO$	$(CH_3)_2CO$	2.008	107	2.29	10
$(CH_3)_2CO$	O_2	2.08	19	2.01	13

[a] In toluene–dichloromethane–L glass at 100–110 K. [b] $\times 10^{-4}$ cm^{-1}.

Table II. Crystallographic Data for $(CH_3OH)_2Co(dmgBF_2)_2$

formula	$CoC_{10}H_{20}B_2F_4N_4O_6$
fw	448.84
space group	$P\bar{1}$
a, Å	7.955 (6)
b, Å	8.180 (6)
c, Å	7.918 (6)
α, deg	99.55 (2)
β, deg	118.13 (2)
γ, deg	66.52 (2)
Z	1
V, Å^3	416.60
d_{calcd}, g/cm^3	1.51
cryst size, mm	0.25 × 0.17 × 0.14
cryst color	red
radiation (λ, Å)	Mo Kα (0.709 26)
μ, cm^{-1}	11.43 (no cor applied)
temp	room temp
2θ limits, deg	2–50
goodness of fit (GOF[a])	1.34
no. of data collcd	1612
no. of unique data	1595
no. of data used in refinement	1027 ($\lvert F_o\rvert \geq 3\sigma(F_o)$)
R^b	0.045
R_w^c	0.046

[a] GOF = $\{\sum w(\lvert F_o\rvert - \lvert F_c\rvert)^2/(NO - NV)\}^{1/2}$, where NO = number of observations and NV = number of variables. [b] $R = \sum\lvert\lvert F_o\rvert - \lvert F_c\rvert\rvert/\sum\lvert F_o\rvert$. [c] $R_w = \{\sum w(\lvert F_o\rvert - \lvert F_c\rvert)^2/\sum wF_o^2)^{1/2}$.

duced cell and reduced cell scalars indicated no transformation to a higher symmetry. All data collected were unique and within a 2θ sphere of 50° in the hkl, $hk\bar{l}$, $h\bar{k}l$, and $h\bar{k}\bar{l}$, octants. The intensity data were corrected for the Lorentz and polarization but not for the absorption effects. The space group was determined as $P\bar{1}$ by a successful refinement. Direct methods and the automated map analysis approach built around MULTAN[18] were used to obtain a trial structure. Full-matrix least-squares refinement was done by minimizing the function $\sum w(\lvert F_o\rvert - \lvert F_c\rvert)^2$, $w = \sigma_F^{-2}$, using anisotropic thermal parameters for non-hydrogen atoms and fixed isotropic thermal parameters for the hydrogen atoms. The refinement converged to a conventional residual index of $R = 4.5\%$ and a weighted residual index of $R_w = 4.6\%$. Additional crystallographic data are presented in Table II.

Results

Spectroscopic and Magnetic Data. The UV/visible spectrum of $(H_2O)_2Co(dmgBF_2)_2$, shown in Figure 1, is characterized by absorption maxima at 456, 328, and 260 nm with molar absorptivities of 4.06×10^3, 1.92×10^3, and 5.82×10^3 M^{-1} cm^{-1}, respectively. The former is particularly characteristic and, owing to its position and intensity, is most often of use in kinetics and other determinations. In contrast, the cobalt(III) complex $(H_2O)_2Co(dmgBF_2)_2^+$ has a relatively weak and featureless visible spectrum, with an intensity that rises into the UV toward the general cobaloxime-type absorption at ca. 260 nm. The magnetic susceptibility of $(H_2O)_2Co(dmgBF_2)_2$ is 1.92 ± 0.02 μ_B at ambient temperature.

The EPR spectra of $L_2Co(dmgBF_2)_2$ are in excellent agreement with those of the close analogue derived from diphenylglyoxime, $L_2Co(dpgBF_2)_2$.[15a,b] The spectra are also very similar to those of other cobalt(II) macrocycles.[19,20] Figures 2 and 3 depict spectra for the complexes with L = acetonitrile, methanol, and acetone.

Table III. Calculated Bond Distances for $(CH_3OH)_2Co(dmgBF_2)_2$

atom pair	dist, Å	atom pair	dist, Å
Co1–N1	1.882 (4)	Co1–N2	1.873 (4)
Co1–O3	2.264 (4)	N1–O1	1.354 (5)
N1–C1	1.266 (6)	N2–O2	1.361 (5)
N2–O2	1.361 (5)	N2–C3	1.273 (7)
O1–B1	1.483 (7)	O2–B1	1.493 (7)
B1–F1	1.395 (7)	B1–F2	1.357 (7)
O3–C5	1.407 (7)	C1–C2	1.492 (8)
C1–C3	1.473 (7)	C3–C4	1.484 (8)
O3–H3	0.739 (62)	C2–H21	0.936 (71)
C2–H22	0.809 (72)	C2–H23	0.913 (72)
C4–H41	0.826 (68)	C4–H42	0.758 (74)
C4–H43	0.946 (70)	C5–H51	0.966 (67)
C5–H52	0.844 (74)	C5–H53	1.029 (69)

Table IV. Selected Bond Angles in $(CH_3OH)_2(dmgBF_2)_2$

atoms	angle, deg	atoms	angle, deg
N1–Co1–O3	91.17 (16)	N2–Co1–O3	89.36 (16)
Co1–N1–O1	123.65 (29)	Co1–N1–C1	116.20 (33)
Co1–O3–C5	128.04 (37)	Co1–N2–O2	123.78 (30)
N1–O1–B1	114.04 (36)	N2–O2–B1	114.37 (36)
O1–N1–C1	119.76 (39)	O1–C1–C2	93.42 (34)
C2–C1–C3	122.63 (44)	N1–C1–C2	124.64 (46)
N1–C1–C3	112.72 (42)	O1–B1–O2	114.91 (43)
O1–B1–F1	109.37 (42)	O1–B1–F2	106.04 (42)
O2–B1–F1	108.65 (42)	O2–B1–F2	105.33 (41)
F1–B1–F2	112.56 (45)	C1–C3–C4	123.08 (45)

Table I summarizes the EPR parameters.

The reversible binding of molecular oxygen, which does not occur to a measurable extent at ambient temperature, was first observed when an oxygenated aqueous solution of the cobalt(II) complex was cooled in a dry ice/acetone bath. As the temperature decreased, the color of the solution changed from a golden yellow to red. This was reversible, and the golden yellow color was restored when the solution was warmed to room temperature, a cycle that could be repeated indefinitely. Similar results were obtained in an organic solvent such as methanol, acetonitrile, and acetone, wherein the deeper intensity of the red color suggested more extensive binding of O_2. The best spectrum was obtained for $(Me_2CO)Co(dmgBF_2)_2O_2$, as shown in Figure 3. The spectral parameters are also given in Table I.

X-ray Structure of $(CH_3OH)_2Co(dmgBF_2)_2$. The refinement of the diffraction pattern resulted in the determination of the crystal and molecular structure of the complex, which is represented by the ORTEP drawing in Figure 4. This confirms the chemical composition of the ligand and establishes that in the recrystallization procedure methanol replaced the two axial water molecules in the original complex. The molecule is highly symmetric and has C_{2h} point group symmetry. Slight distortions in the macrocyclic ring were detected in the solid-state structure by the X-ray data, which lowered the point group symmetry to C_i (pseudo-C_{2h}). Owing to the inversion center of symmetry, only half of the geometric parameters are independent. Tables III–V give calculated bond distances, selected bond angles, and positional and isotropic thermal parameters.

Reversible Oxidation–Reduction Chemistry of $(H_2O)_2Co(dmgBF_2)_2$. Treatment of the Co(II) complex with a slight excess of $Fe(H_2O)_6^{3+}$ results in a bleaching of the characteristic absorption of the former at 456 nm. As shown in Figure 1, subsequent addition of excess Cr^{2+}, provided it is done quickly enough,[21] restores the Co(II) spectrum to >95% of its original intensity. These observations are consistent with reactions

$$Fe(H_2O)_6^{3+} + (H_2O)_2Co(dmgBF_2)_2 = Fe(H_2O)_6^{2+} + (H_2O)_2Co(dmgBF_2)_2^+ \quad (1)$$

$$(H_2O)_2Co(dmgBF_2)_2^+ + Cr^{2+} = (H_2O)_2Co(dmgBF_2)_2 + Cr^{3+} \quad (2)$$

(18) Main, P.; Woolfson, M. M.; Germain, G. *MULTAN, A Computer Program for the Automated Solution of Crystal Structures*; University of York: York, Great Britain, 1971.
(19) Walker, F. A. *J. Am. Chem. Soc.* **1970**, *92*, 4235.
(20) Hoffman, B. M.; Diemente, D. L.; Basolo, F. *J. Am. Chem. Soc.* **1970**, *92*, 61.

(21) The re-reduction must be done without delay, however, since the Co(III) complex decomposes in acidic solutions; this contrasts with the Co(II) complex, which survives hours in acidic solution, (e.g., $t_{1/2}$ = 9 min and 5.5 h, respectively, at 0.050 M H^+).

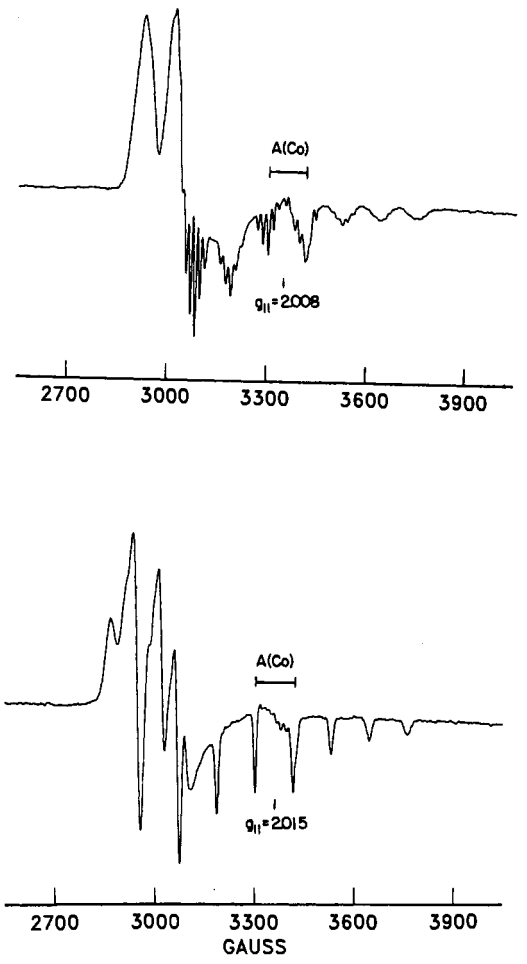

Figure 2. EPR spectra of $L_2Co(dmgBF_2)_2$ for L = CH_3CN (top) and CH_3OH (bottom).

Table V. Atomic Positional and Average Isotropic Thermal Parameters[a] for $(CH_3OH)_2Co(dmgBF_2)_2$

atom	x	y	z	U(av)
Co1	0	0	0	20 (0)
N1	2627 (6)	−1253 (5)	1917 (5)	25 (1)
N2	−1347 (6)	−1415 (5)	30 (5)	24 (1)
O1	3134 (5)	−2815 (4)	2735 (5)	31 (1)
O2	−381 (5)	−2949 (4)	1099 (5)	29 (1)
O3	851 (6)	−1806 (5)	−2197 (5)	38 (2)
C1	4009 (7)	−659 (6)	2288 (7)	23 (2)
C2	6221 (8)	−1544 (8)	3628 (8)	34 (2)
C3	3210 (7)	1012 (6)	1221 (7)	25 (2)
C4	4451 (10)	2109 (8)	1605 (9)	37 (3)
C5	1616 (11)	−3681 (8)	−2198 (11)	45 (3)
B1	1444 (9)	−2969 (8)	2941 (9)	28 (2)
F1	811 (5)	−1588 (4)	4058 (4)	37 (1)
F2	2208 (5)	−4603 (4)	3758 (4)	39 (1)
H21	644 (10)	−245 (9)	437 (9)	38
H22	686 (11)	−212 (9)	304 (9)	38
H23	667 (11)	−66 (9)	429 (9)	38
H3	−941 (9)	−141 (8)	−311 (9)	38
H41	477 (10)	250 (8)	270 (10)	38
H42	547 (11)	158 (9)	159 (10)	38
H43	−362 (10)	−309 (9)	−73 (9)	38
H51	−108 (10)	−568 (9)	178 (10)	38
H52	−714 (11)	−412 (9)	−196 (10)	38
H53	−91 (11)	−563 (9)	334 (10)	38

[a] Atomic coordinates (× 10^4), temperature factors [$Å^2$ × 10^3]; U(av) is the average of U_{11}, U_{22}, and U_{33}.

The extent of oxidation of $(H_2O)_2Co(dmgBF_2)_2$ by $Fe(H_2O)_6^{3+}$ is also affected by the $Fe(H_2O)_6^{3+}$ and $Fe(H_2O)_6^{2+}$ concentrations, increasing with the former and decreasing with the latter. This indicates that the reaction written in eq 1 is a balanced chemical

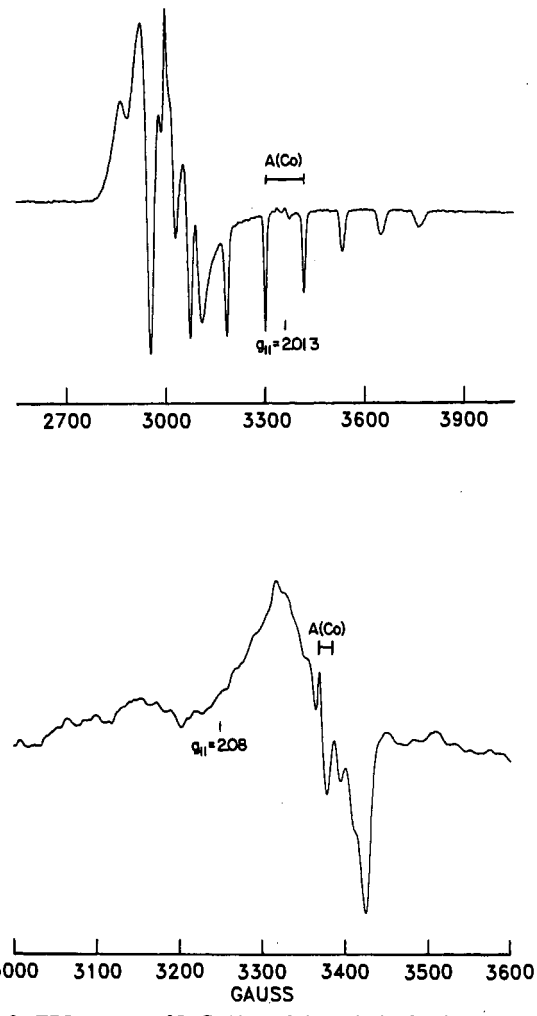

Figure 3. EPR spectra of $L_2Co(dmgBF_2)_2$ and of $LCo(dmgBF_2)_2O_2$ for L = $(CH_3)_2CO$.

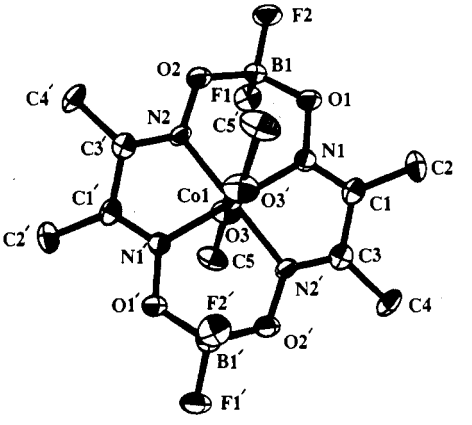

Figure 4. Full ORTEP drawing of the molecular structure of $(CH_3OH)_2Co(dmgBF_2)_2$. The hydrogen atoms are not included in the ORTEP drawing for clarity, and the thermal ellipsoids are drawn at 50% probability.

equilibrium and that the Co(III)/Co(II) couple is comparable to Fe^{3+}/Fe^{2+} in oxidation–reduction strength. Cyclic voltammetry and numerical measurements of the equilibrium constant and rate constants for eq 1 serve to confirm that interpretation.

Cyclic Voltammetry. The Co(II)/Co(I) redox couple is nearly reversible. At scan rates <1000 mV/s in 0.10 M $LiClO_4$, plots of the peak currents vs. the square root of the scan velocity are linear and the peak separations are 70–90 mV. The hanging-mercury-drop and glassy-carbon electrodes produced the best voltammograms for the Co(II)/Co(I) couple, and defined $E_{1/2}$ = −0.434 V vs. NHE at 25 °C. Plots of i_{pa}/i_{pc} vs. scan rate indicate

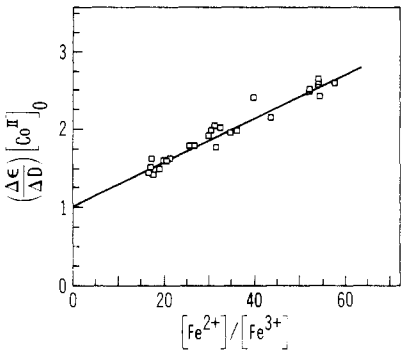

Figure 5. Equilibrium constant for oxidation of $(H_2O)_2Co(dmgBF_2)_2$ by Fe^{3+} determined from the slope of a plot related to eq 3. The line corresponds to the least-squares fit of the data and yields $K_{eq} = 34.7 \pm 2.9$ at 0.50 M ionic strength and 25 °C.

slight electrochemical irreversibility, owing to partial decomposition of the Co(I) species according to an EC mechanism:[22]

$$E: \quad Co(dmgBF_2)_2 + e^- = Co(dmgBF_2)_2^-$$

$$C: \quad Co(dmgBF_2)_2^- + H_2O = {}^1/_2H_2 + Co(dmgBF_2)_2 + OH^-$$

The Co(III)/Co(II) couple appears to be quasi-reversible at best, since the peak separation increases with increasing scan rate. This is probably due to sluggish electron transfer at the electrode surface, which is relatively less important for the Co(II)/Co(I) couple. The best results were obtained for the glassy-carbon electrode in lithium perchlorate solutions. We estimate $E_{1/2} = 0.683$ V, vs. NHE at 25 °C in 0.1 M $LiClO_4$.

Equilibrium Constant. The value of K_{eq} for eq 1 was determined by two independent methods. First and more precisely, spectrophotometric measurements at λ 456 nm were made on solutions prepared by using known concentrations of $(H_2O)_2Co(dmgBF_2)_2$, Fe^{3+}, and Fe^{2+}. (The last two are in considerable excess over the first, so that changes in concentrations of Fe^{3+} and Fe^{2+} from their added values are small.) The difference between the final and initial absorbances, ΔD, can be related to the concentrations of the species present, their molar absorptivities, ϵ, and K_{eq} by

$$\frac{\Delta\epsilon}{\Delta D}[Co(II)]_0 = \frac{[Fe^{2+}]_{eq}}{K_{eq}[Fe^{3+}]_{eq}} + 1 \qquad (3)$$

These measurements were conducted at various acid concentrations in the range $0.1 < [H^+] < 0.5$ M; no effect of $[H^+]$ was observed. A linear plot suggested by eq 3 is shown in Figure 5. A least-squares analysis gives $K_{eq} = 34.7 \pm 2.9$ at 0.50 M ionic strength and 25.0 °C.

A second value of K_{eq} is obtained from the quotient of the forward and reverse constants, evaluated as described in the next section. Application of this method to data at $[H^+] = 0.40$ M affords $K_{eq} = 31.4 \pm 3.4$ under the same conditions. The agreement between the two is within experimental error and suggests that the system is properly characterized by the single equilibrium reaction. The former value of K_{eq} is the more direct and presumably more accurate, and we adopt it in the subsequent analysis.

Kinetics. Two types of measurements were made, one based on conventional spectrophotometry at relatively high $[H^+]$, 0.40 M, where the reaction rates are lower, and the other using the stopped-flow technique. The former data emphasized the reversible nature of the reaction and entailed use of added Fe^{2+}, so as to cause appreciable amounts of reactants to remain at equilibrium. The latter used higher $[Fe^{3+}]$, which caused the reaction to go essentially to equilibrium, and lower $[H^+]$, which caused an acceleration in the rate.

(22) Nicholson, R. S.; Shane, I. *Anal. Chem.* **1964**, *36*, 706.

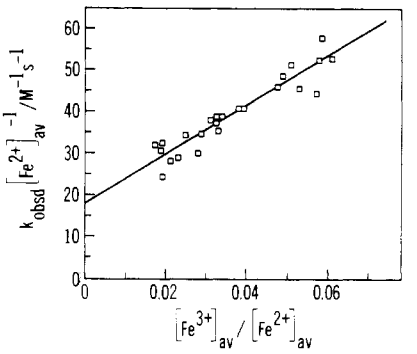

Figure 6. Kinetic data for the oxidation of $(H_2O)_2Co(dmgBF_2)_2$ by Fe^{3+} at 0.400 M H^+ obtained under conditions where the reaction is reversible. The rate constant for the approach to equilibrium, k_{obsd}, is related to concentrations by eq 4; the data are plotted here in a linear fashion. The least-squares rate constants, both refined independently, are $k_f = 575 \pm 45$ M^{-1} s^{-1} and $k_r = 18.3 \pm 1.8$ M^{-1} s^{-1} (at 0.50 M ionic strength and 25.0 °C).

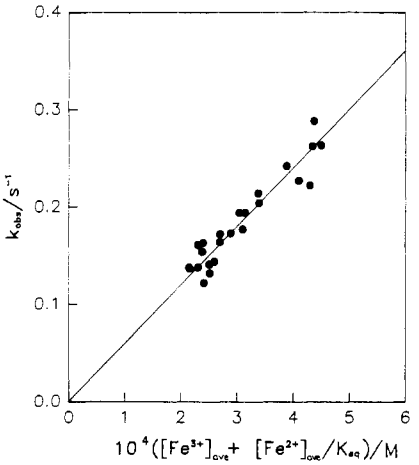

Figure 7. Same kinetic data as shown in Figure 5 analyzed as suggested by eq 5, with the ratio k_f/k_r constrained to match the independently known value of K_{eq}. This least-squares fit yields $k_f = 599 \pm 10$ M^{-1} s^{-1} and $k_r = 17.3 \pm 0.3$ M^{-1} s^{-1}.

The rate constant for approach to equilibrium in the first set of experiments is that for a pair of opposing pseudo-first-order reactions:

$$k_{obsd} = k_f[Fe^{3+}] + k_r[Fe^{2+}] \qquad (4)$$

Figure 6 shows a plot of the data at $[H^+] = 0.400$ M as $k_{obsd}/[Fe^{2+}]$ vs. $[Fe^{3+}]/[Fe^{2+}]$, as suggested by eq 4. This analysis yields $k_f = 575 \pm 45$ M^{-1} s^{-1} and $k_r = 18.3 \pm 1.8$ M^{-1} s^{-1}. Alternatively, the data from these runs can be analyzed with the restraint that the ratio k_f/k_r be equal to the best value of K_{eq}, as previously determined. Rearrangement of eq 4 with that restraint yields the equation

$$k_{obsd} = k_f\{[Fe^{3+}] + [Fe^{2+}]K_{eq}^{-1}\} \qquad (5)$$

With K_{eq} set at 34.7, the use of eq 5 (Figure 7) gives $k_f = 599 \pm 10$ M^{-1} s^{-1}. The reverse rate constant is given as $k_f/K_{eq} = 17.3 \pm 0.3$ M^{-1} s^{-1}. These values apply to a single $[H^+] = 0.400$ M at 0.50 M ionic strength and 25.0 °C.

The second and more extensive set of data was determined at higher $[Fe^{3+}]$ without added Fe^{2+}, such that the reaction proceeded essentially to completion. In those circumstances, only the forward rate contributes appreciably to the observed reaction rate. In keeping with that, at each $[H^+]$ the reaction is found to proceed to completion, and a plot of k_{obsd} vs. $[Fe^{3+}]$ is linear and passes through the origin. The slope of such a plot at each $[H^+]$ affords an apparent second-order rate constant designated k_f^{app} for the forward reaction. These values increase with decreasing $[H^+]$

Table VI. Bond Lengths, Magnetic Susceptibilities, and Standard Reduction Potentials of Cobalt(II) Macrocyclic Complexes

complex[a]	eq M–N, Å: amine	eq M–N, Å: imine	ax M–O, Å	μ_{eff}, μ_B	$E°$,[a] V
$[(H_2O)_2Co(dmgBF_2)_2]$[b]		1.88	2.27	1.92	0.649
$[(H_2O)_2Co(Me_4[14]tetraeneN_4)](ClO_4)_2$[c]		1.90	2.29	1.82	0.564[d]
$[(H_2O)_2Co(Me_2[14]1,11\text{-dieneN}_4\text{-}13\text{-one})](ClO_4)_2$[e]	1.98	1.92	2.28, 2.39		0.600[d]
$[(H_2O)_2Co(Me_6[14]4,11\text{-dieneN}_4)](BF_4)_2$[f]	1.98	1.92	2.48	1.86	0.564[d]
$[(H_2O)Co(Me_2[14]4,7\text{-dieneN}_4)](PF_6)_2$[g]	1.99	1.92	2.28	2.05	
$[(H_2O)Co(Me_2pyo[14]trieneN_4)](ClO_4)_2$[h]				2.03	0.567
$[(H_2O)_2Co(dmgH)_2]$				1.82[i]	0.36[j]

[a] $Co^{III/II}$ reduction potential. [b] This work; structural data refer to $[(CH_3OH)_2Co(dmgBF_2)_2]$. [c] Reference 27. [d] Reference 25. [e] Reference 28. [f] Reference 27. [g] Reference 24. [h] Reference 30. [i] Sharpe, A. G.; Wakefield, D. B. *J. Chem. Soc.* **1957**, 281. [j] Reference 35.

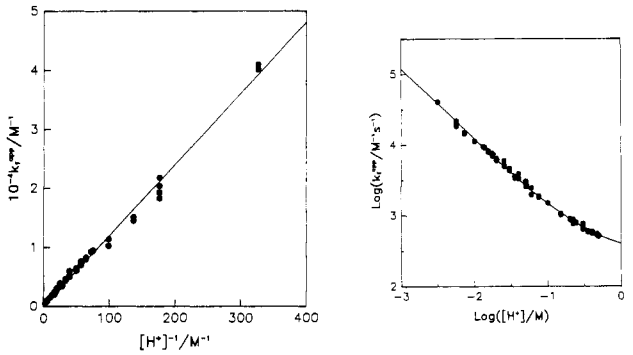

Figure 8. $[H^+]$-dependence of the forward rate constant for the reaction between $(H_2O)_2Co(dmgBF_2)_2$ and Fe^{3+} shown as k_f^{app} (see eq 6) vs. $[H^+]^{-1}$ on a linear scale (left) and as a log–log relation (right). The solid curves drawn in both graphs correspond to the weighted least-squares fit of the data to eq 6.

and describe an algebraic relation[23] such that k_f^{app} varies linearly with $[H^+]^{-1}$:

$$k_{obsd}/[Fe^{3+}] = k_f^{app} = A + B/[H^+] \quad (6)$$

The data plotted in this fashion are shown in Figure 8a, and the same results are shown on logarithimic scales in Figure 8b. In both representations there is a solid line that represents the least-squares-fit values of the two kinetic parameters, $A = 289 \pm 11\ M^{-1}\ s^{-1}$ and $B = 120 \pm 2\ s^{-1}$.

Discussion

Spectroscopic and Structural Features of $(H_2O)_2Co(dmgBF_2)_2$. Most cobalt(II) complexes of nonmacrocyclic tetradentate ligands with nitrogen and/or oxygen donors are high-spin, five- or six-coordinate complexes.[24] Many tetradentate macrocycles, on the other hand, have sufficiently high ligand fields to stabilize cobalt(II) in a low-spin environment. A number of 14-membered tetraaza macrocyclic complexes of cobalt(II) have low-spin configurations. These d^7 complexes exist in high ligand fields, have magnetic susceptibilities that are near the spin-only value for a single unpaired electron, and have six-coordinate structures with oxygen donors, often water molecules, in their axial positions at longer-than-normal Co–O bond distances.[25-30]

The complex $(H_2O)_2Co(dmgBF_2)_2$ falls in the same category. Its characteristics, summarized in Table VI, are quite comparable to those of cobalt(II) complexes of similar composition. Its magnetic moment of 1.92 μ_B is only slightly larger than the spin-only value, 1.73 μ_B; this is comparable to those of the other complexes but distinctly different from the values expected (spin-only, 3.46 μ_B) and found (typically 4.9–5.2 μ_B) for high-spin Co(II).

The EPR spectra of frozen toluene–dichloromethane–ligand solutions indicate a nearly axial symmetry about the cobalt(II). This result is consistent with the known electronic structures of low-spin Co(II) complexes, with a d^7 electronic configuration and one unpaired electron in the d_{z^2} orbital.

It is difficult to assign unambiguously the EPR spectrum of the O_2 adducts $LCo(dmgBF_2)_2O_2$ when the donor atom of L lacks a nuclear spin, as is the case at hand, since EPR hyperfine splitting cannot be observed. This was overcome[15] for the closely related complex $L_2Co(dpgBF_2)_2$ by noting the change in the spectrum as L = CH_3CN was replaced by THF and then by O_2. On the basis of those data, it is clear that six-coordination is preserved during oxygen binding.

The strong electron-withdrawing character of the macrocycle when BF_2 groups are incorporated into the macrocycle is apparent when comparisons are made with the parent complex $Co(dmgH)_2$. This effect is manifest in the reduction potentials that tend to stabilize the respective lower oxidation states by ~0.3 V and in the greatly reduced tendency to bind O_2.

It has been observed that the axial bond lengths dramatically depend on spin state. The axial Co^{II}–OH_2 bond is susceptible to nonbonded repulsive interactions with substituents on the equatorial macrocycle but increases in strength with increased unsaturation in the macrocycle. The data collected in Table VI illustrate these assertions: The equatorial Co–N(imine) and Co–N(amine) bond lengths are constant, 1.92 ± 0.02 and 1.98 ± 0.01 Å, respectively. The axial Co–O bond lengths vary from 2.27 to 2.48 Å, as a direct result of the Jahn–Teller effect in low-spin d^7 complexes. The extent to which the latter range really does represent an elongation beyond the "normal" distance can be seen from the values found for high-spin Co(II) complexes: aquo(*N,N'*-ethylenebis(3-methoxysalicylideneaminato))cobalt(II) (2.12 Å),[31] CoO(s) (2.13 Å),[32] $CoCl_2 \cdot 6H_2O$ (2.12 Å),[33] and an "accepted" average Co(II)–O bond distance of 2.14 ± 0.10 Å.[33] The Co–N(imine) equatorial and Co–O axial bond lengths determined for $(CH_3OH)_2Co(dmgBF_2)_2$, 1.88 and 2.27 Å, respectively, agree well with values for similar complexes in Table VI. The axial lability in the low-spin cobalt(II) complexes, which is vital to their ability to react by efficient inner-sphere mechanisms, arises from the axial elongation.[27]

Electron Transfer: Equilibrium and Mechanism. The equilibrium constant for eq 1, when combined with $E°$ for Fe^{3+}/Fe^{2+}

(23) This analysis of the functional form of the $[H^+]$-dependence of the kinetic data is the most successful of several attempted. It results in an average deviation of 4.6% between experimental and calculated values of k_{obsd} and a maximum deviation of 17.0%. In contrast, the alternative form where $k_f^{app} = C/\{D + [H^+]\}$ is far more inferior with 14.6% deviation on average and 45.3% at the worst. As a consequence of the poor fit, the latter analysis will not be detailed here.

(24) Roberts, G. W.; Cummings, S. C.; Cunningham, J. A. *Inorg. Chem.* **1976**, *15*, 2503.
(25) Endicott, J. F.; Durham, B.; Glick, M. D.; Anderson, T. J.; Kuszaj, J. M.; Schmonsees, W. G.; Balakrishnan, K. P. *J. Am. Chem. Soc.* **1981**, *103*, 1431.
(26) Tait, A. M.; Busch, D. H. *Inorg. Chem.* **1976**, *15*, 197.
(27) Endicott, J. F.; Lilie, J.; Kuszaj, J. M.; Ramaswamy, B. S.; Schmonsees, W. G.; Simic, M. S.; Glick, M. D.; Rillema, J. A. *J. Am. Chem. Soc.* **1977**, *99*, 429.
(28) Durham, B.; Anderson, T. J.; Switzer, J. A.; Endicott, J. F.; Glick, M. D. *Inorg. Chem.* **1977**, *16*, 271.
(29) Glick, M. D.; Schmonsees, W. G.; Endicott, J. F. *J. Am. Chem. Soc.* **1974**, *96*, 5661.
(30) Long, K. M.; Busch, D. H. *Inorg. Chem.* **1970**, *9*, 505.
(31) Calligaris, M.; Nardin, G.; Randaccio, L. *J. Chem. Soc., Dalton Trans.* **1974**, 1903.
(32) MacGillavry, C. H.; Fieck, G. D. *International Tables for X-Ray Crystallography*; Kynoch: Birmingham, Great Britain, 1962; Vol. III.
(33) Wyckoff, R. W. G. *Crystal Structures*; Wiley: New York, 1965; Vol. 3.

(0.740 V at 0.500 M ionic strength and 25.0 °C)[34] affords the value $E^\circ = 0.649 \pm 0.003$ V for the $(H_2O)_2Co(dmgBF_2)_2^+/(H_2O)_2Co(dmgBF_2)_2$ couple. This is clearly more positive than many other values (Table VII), including the value 0.36 V for the parent cobaloxime.[35] The lower reducing strength of $(H_2O)_2Co(dmgBF_2)_2$ is consistent with the BF_2 substituent being electron-withdrawing.

The mechanism suggested by eq 6 allows us to infer that the reaction occurs by parallel bimolecular paths. The minor $[H^+]$-independent pathway (parameter A) represents the direct reaction between $Fe(H_2O)_6^{3+}$ and $(H_2O)_2Co(dmgBF_2)_2$ and the other (parameter B) that between $(H_2O)_5FeOH^{2+}$ and $(H_2O)_2Co(dmgBF_2)_2$. In the latter case the bimolecular rate constant, given by B/K_a^{Fe}, is 6.2×10^4 M^{-1} s^{-1}. The high reactivity of $FeOH^{2+}$ suggests that this reaction, like so many others,[36-39] proceeds by an inner-sphere, hydroxide-bridged transition state. A $[H^+]$-independent rate law is expected for an outer-sphere mechanism. A pertinent example is the $[H^+]$-independent oxidation of the macrobicyclic complex $Co(sep)^{2+}$ by Fe^{3+}.[40]

In that event, a more detailed analysis of the kinetic parameters can be made. To assist in the analysis, eq 7–12 show the parallel

$$Fe(H_2O)_6^{3+} = (H_2O)_5FeOH^{2+} + H^+ \quad (K_a^{Fe}) \quad (7)$$

$$Fe^{3+} + (H_2O)_2Co(dmgBF_2)_2 \rightleftarrows Fe^{2+} + (H_2O)_2Co(dmgBF_2)_2^+ \quad (k_1, k_{-1}) \quad (8)$$

$$FeOH^{2+} + (H_2O)_2Co(dmgBF_2)_2 \rightleftarrows [Fe^{III}(OH)Co^{II}(dmgBF_2)_2(H_2O)]^{2+} \quad (k_2, k_{-2}) \quad (9)$$

$$[Fe^{III}(OH)Co^{II}]^{2+} \rightleftarrows [Fe^{II}(OH)Co^{III}(dmgBF_2)_2(H_2O)]^{2+} \quad (k_3, k_{-3}) \quad (10)$$

$$[Fe^{II}(OH)Co^{III}(dmgBF_2)_2(H_2O)] \rightleftarrows Fe^{2+} + (H_2O)(OH)Co(dmgBF_2)_2 \quad (k_4, k_{-4}) \quad (11)$$

$$(H_2O)_2Co(dmgBF_2)_2^+ = (H_2O)(OH)Co(dmgBF_2)_2 + H^+ \quad (K_a^{Co}) \quad (12)$$

path reaction scheme in more detail, separating the contributions of precursor complex formation, intramolecular electron transfer, and successor complex dissociation. Furthermore, since the reaction is fully reversible, it becomes useful to consider the values and implications of the kinetic parameters for the reverse transformation, which are also determined by this experimental study.

In terms of these rate constants, the kinetic parameters for the forward reaction determined experimentally are $A = k_1$ and $B = k_2k_3K_a^{Fe}/(k_{-2} + k_3)$. When it is assumed that intramolecular electron transfer is the rate-limiting step in the inverse-acid path, i.e., $k_{-2} \gg k_3$, the latter simplifies to $B \sim k_2k_3K_a^{Fe}/k_{-2}$. The parameters for the reverse reaction, calculated from the equilibrium constant by application of the principle of microscopic reversibility, are expressed as $k_{-1} = A/K_{eq}$ and $B/K_{eq} = k_{-4}k_{-3}K_a^{Co}/(k_4 + k_{-3})$, with the latter given approximately by $k_{-4}k_{-3}K_a^{Co}/k_4$. Numerical values are $A = k_1 = (2.89 \pm 0.11) \times 10^2$ M^{-1} s^{-1}, $B = (1.20 \pm 0.02) \times 10^2$ s^{-1}, $k_{-1} = 8.3 \pm 1.0$ M^{-1} s^{-1}, and $B/K_{eq} = k_{-4}k_{-3}K_a^{Co}/k_4 = 3.5 \pm 0.3$ s^{-1}.

When additional values or estimates are used, still further detail can be obtained. For example, $K_a^{Fe} = 1.94 \times 10^{-3}$ M at this ionic strength and temperature.[41] With that value, $k_2k_3/k_{-2} = (6.2 \pm 0.1) \times 10^4$ M^{-1} s^{-1}. With an assumed approximate value of $K_a^{Co} \sim 10^{-5}$ M for the acid ionization constant of $(H_2O)_2Co(dmgBF_2)_2^+$,[42] $k_{-4}k_{-3}/k_4 \simeq 3.5 \times 10^4$ M^{-1} s^{-1}.

The bimolecular rate constants necessarily lie below the diffusion-controlled limit, or $k_2, k_{-4} < 10^{10}$ M^{-1} s^{-1}. The unimolecular rate constants k_{-2} and k_4 represent the rates of ligand dissociation from Co(II) macrocycles and $Fe(H_2O)_6^{2+}$, respectively. From the known rates of water exchange we estimate $k_{-2} \sim 10^9$ s^{-1} [27] and $k_4 \sim 10^{6.5}$ s^{-1}.[43] This sets lower limits on the rate constants k_3 and k_{-3} for the rate-limiting intramolecular electron-transfer step: $k_3 > 6.2 \times 10^3$ s^{-1} and $k_{-3} > 40$ s^{-1}. Their upper limits are given from the inequalities that govern their being the rate-limiting step, or $k_3 < 10^9$ s^{-1} and $k_{-3} < 10^7$ s^{-1}. The assumptions used in deriving these limits have all been stated; they are reasonable chemically, considering what is known independently about the chemistry of the individual reaction types, and are internally consistent as well.

Acknowledgment. The principal support for this research was provided by the National Science Foundation (Grant CHE-8418084). We gratefully acknowledge J. E. Benson, S. Kim, and L. Miller for assistance with the X-ray structural determination and S. L. Bruhn, B. M. Hoffman, and L. Pearce for assistance with the EPR measurements.

Registry No. $(H_2O)_2Co(dmgBF_2)_2$, 91443-37-7; $(CH_3OH)_2Co(dmgBF_2)_2$, 104422-06-2; $Fe(H_2O)_6^{3+}$, 15377-81-8; $(H_2O)_2Co(dmgBF_2)_2^+$, 104422-07-3; $(CH_3CN)_2Co(dmgBF_2)_2$, 104422-08-4; $((CH_3)_2CO)_2Co(dmgBF_2)_2$, 104422-09-5; $((CH_3)_2CO)(O_2)Co(dmgBF_2)_2$, 104438-48-4; Cr^{2+}, 22541-79-3; $(H_2O)_2Co(dmgBF_2)_2^-$, 104422-10-8.

Supplementary Material Available: Full listings of bond angles and anisotropic thermal parameters (5 pages); a listing of observed and calculated structure factors (3 pages). Ordering information is given on any current masthead page.

(34) Weaver, M. J.; Nettles, S. M. *Inorg. Chem.* **1980**, *19*, 1641.
(35) Espenson, J. H.; Heckman, R. A. *Inorg. Chem.* **1979**, *18*, 38.
(36) Cannon, R. D. *Electron Transfer*; Butterworths: London, 1980; pp 137–161.
(37) Wilkins, R. G. *The Study of Kinetics and Mechanism of Reactions of Transition Metal Complexes*; Allyn and Bacon: Boston, 1974; pp 255–274.
(38) Dulz, G.; Sutin, N. *J. Am. Chem. Soc.* **1964**, *86*, 829.
(39) Carlyle, D. W.; Espenson, J. H. *J. Am. Chem. Soc.* **1968**, *90*, 2272.
(40) Rudgewick-Brown, N.; Cannon, R. D. *Inorg. Chem.* **1985**, *24*, 2463.
(41) Milburn, R. M.; Vosburgh, W. C. *J. Am. Chem. Soc.* **1955**, *77*, 1352.
(42) The acid ionization constant reported for $(H_2O)_2Co(dmgH)_2^+$ is 7.2×10^{-6} M [Costa, G. *Pure Appl. Chem.* **1972**, *30*, 344]. Considering the strong electron-withdrawing effect of the BF_2 substituents in the modified macrocycle, we make an approximate estimate (±1 pK_a unit) of $K_a^{Co} \sim 10^{-5}$ M.
(43) Swift, T. J.; Connick, R. E. *J. Chem. Phys.* **1962**, *37*, 307.